



島根大学学術情報リポジトリ
S W A N
Shimane University Web Archives of kNowledge

Title

Unusual Nonmagnetic Ordered State in CeCoSi Revealed by ^{59}Co -NMR and NQR Measurements

Author(s)

Masahiro Manago, Hisashi Kotegawa, Hideki Tou, Hisatomo Harima, and Hiroshi Tanida

Journal

Journal of the Physical Society of Japan Volume 90, Number 2

Published

January 18, 2021

URL

<https://doi.org/10.7566/JPSJ.90.023702>

この論文は出版社版ではありません。
引用の際には出版社版をご確認のうえご利用ください。

Unusual Nonmagnetic Ordered State in CeCoSi Revealed by ^{59}Co -NMR and NQR Measurements

Masahiro Manago,* Hisashi Kotegawa, Hideki Tou, and Hisatomo Harima
Department of Physics, Kobe University, Kobe, Hyogo 657-8501, Japan

Hiroshi Tanida

Liberal Arts and Sciences, Toyama Prefectural University, Imizu, Toyama 939-0398, Japan

Abstract

We performed ^{59}Co nuclear magnetic and quadrupole resonance (NMR and NQR) measurements under pressure on a single-crystalline CeCoSi, which undergoes an unresolved phase transition at T_0 . The NQR spectra clearly showed that the phase transition at T_0 is nonmagnetic, but any symmetry lowering at the Co site was not seen irrespective of the feature of second-order phase transition. By contrast, the NMR spectra were split by the induced magnetic field perpendicular to the external magnetic field. These results show that the phase below T_0 is not a simple paramagnetic state but is most likely electric multipolar ordered state of Ce $4f$ electrons. The development of the Kondo effect by applying pressure is thought to be crucial to stabilize this state and to show novel features beyond commonality of tetragonal Ce-based systems.

Physical properties of solids are influenced intricately by degrees of freedom of electrons, that is, charge, spin, and orbital, through their mutual couplings and many-body interactions of electrons. Phase transition characterized by an order parameter is one of the demonstrations of their influence; therefore, it is a fundamental yet profound phenomenon. Rich interactions in solids induce various types of phase transitions; hence, they are attractive in condensed matter physics.

Such diversity yields at times a mysterious ordered state. A well-known example is the “hidden order” state in the $5f$ -electron system URu_2Si_2 [1, 2]. It is a second-order phase transition with a symmetry reduction; however, the crystallographic symmetry of the ordered state is still controversial [3–6]. Several researchers have attempted unmasking the order parameter in URu_2Si_2 for three decades because it is just a fundamental question in condensed matter physics; the mechanism through which degrees of freedom of electrons can affect physical properties of solids.

The $4f$ -electrons system CeCoSi is a potential example exhibiting an extraordinary order parameter. It crystallizes in the tetragonal $P4/nmm$ (D_{4h}^7 , No. 129) space-group symmetry with the CeFeSi -type structure [7]. The spacial inversion symmetry is locally absent at the Ce site, whereas the crystal structure has the global inversion symmetry. The crystal electric field (CEF) ground state has been reported as the Γ_7 ($\mp 0.306 |\pm 5/2\rangle \pm 0.95 |\mp 3/2\rangle$) Kramers doublet, and the first excited state is separated from it by ~ 100 K [8]. It has been established that an antiferromagnetic (AFM) transition occurs at the Néel temperature $T_N = 9.4$ K. The transition is of second-order [9], and the Ce moments with sizes of $m_{\text{Ce}} \sim 0.37(6)\mu_B$ are aligned along the $[100]$ axis with a $\mathbf{q} = \mathbf{0}$ structure, as revealed by a neutron scattering study [8]. Another phase, which is a matter of interest, has been initially reported to emerge under pressure below ~ 40 K at ~ 1.5 GPa [10]. The first unresolved issue of this phase is its intrinsic pressure phase diagram. Contrary to some reports [8, 10], a study on single-crystalline samples proposed that this “pressure-induced ordered phase” already exists at ambient pressure below $T_0 = 12$ K [11]. The phase below T_0 at lower pressures seems to continuously connect to the pressure-induced phase [11, 12]. However, the anomaly at T_0 at ambient pressure is not sufficiently large to convince a phase transition. Therefore, microscopic measurements are desired to reveal whether the phase transition at T_0 is intrinsic or not at ambient pressure. The second unresolved issue is the order parameter below T_0 . It seems different from usual AFM states, as deduced from an enhancement by the magnetic field [10, 11]. There have been various suggestions for the origin of this phase, as follows: the spin-density-wave order of Co $3d$ electrons, metaorbital transition, and antiferroquadrupolar (AFQ) ordering [10–12]; however, the order parameter remains unresolved.

In this Letter, we present the results of ^{59}Co nuclear magnetic and quadrupole resonance (NMR and NQR) measurements on high-quality single-crystalline CeCoSi samples to clarify the above-mentioned issues. The combined NMR and NQR results revealed the intrinsic phase diagram, where the objective phase was present even at ambient pressure. In the ordered state, there is no clear indication of symmetry reduction at the Co site under zero field, whereas the NMR spectra split below T_0 when the magnetic field tilted from the [100] axis was applied. This NMR anomaly can be interpreted by the emergence of the induced magnetic field perpendicular to the external field. Present results suggest an unusual nonmagnetic ordered state that is most likely an electric multipole ordered state in CeCoSi.

Plate-shaped single-crystalline CeCoSi samples ($\sim 3 \times 4 \times 0.5 \text{ mm}^3$) were grown using the Ce/Co eutectic flux method, as described in Ref. 11. The ^{59}Co ($I = 7/2$) NMR and NQR measurements were performed in the temperature range 1.4–300 K using a standard spin-echo method. The NMR spectra were obtained under a field of 1 T near the [100] direction, and its angle was deduced from the frequencies of the spectra above T_0 . The local symmetry of the Co site in the $P4/nmm$ space group is $\bar{4}m2$ with four-fold improper rotational symmetry. Hydrostatic pressure was applied up to 2.35 GPa on another sample using a piston-cylinder-type cell with Daphne 7474 as a pressure-transmitting medium. The pressure was determined from the superconducting transition temperature of a Pb sample inside the cell. A LaCoSi sample consisting of single-crystalline pieces was also measured by NQR at $P = 0$ as a reference system.

The NQR spectra are sensitive to both the magnetic and electric anomalies and are suitable for probing the nature of the ordered state. Figures 1(a)–1(c) show the temperature dependence of the NQR spectra above T_N at the $\nu_3 \equiv 3\nu_Q$ ($\pm 5/2 \leftrightarrow \pm 7/2$) site at 0, 1.09, and 1.52 GPa. The value of the quadrupole frequency ν_Q was 2.09 MHz at $P = 0$ and 20 K. The results on other pressures are shown in the Supplemental Materials [13]. The NQR spectra did not split nor broaden, although they showed a shift at T_0 . As shown in the temperature dependence of ν_Q in Fig. 1(d), the kink of ν_Q is clearer at higher pressures, and it is invisible at ambient pressure. The kink is not a necessary condition for the phase transition, and its presence at ambient pressure is proved by NMR measurements mentioned later. The absence of splitting or broadening NQR spectra demonstrates that the internal field is absent at the Co sites for $T_N < T < T_0$ in the entire pressure range. This clearly excludes the magnetic ordering of Co $3d$ moments below T_0 . Our results also indicate that all the Co sites remain equivalent below T_0 while maintaining a local tetragonal symmetry, that is, a tetragonal crystal structure [13]. If one considers a possibility of

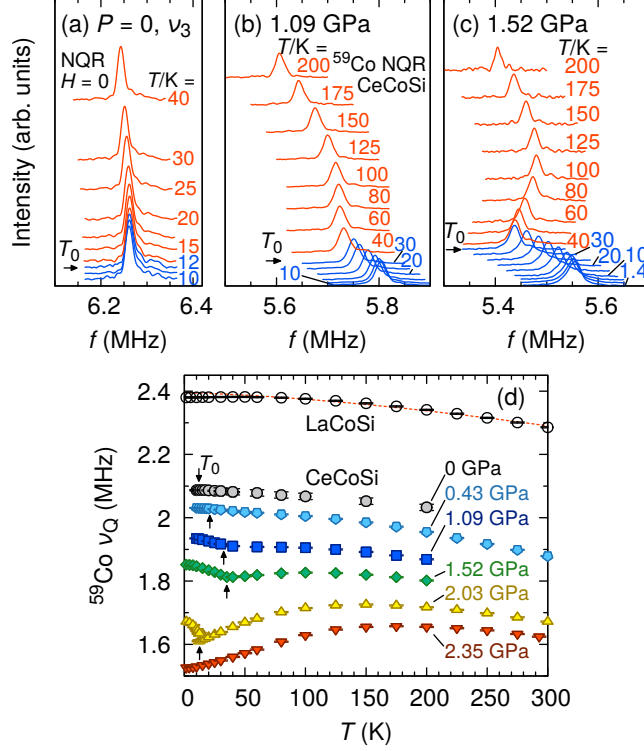


FIG. 1. (Color online) (a–c) Temperature dependence of the ^{59}Co NQR spectra of CeCoSi at $\nu_3 \equiv 3\nu_Q$ site without a field under a pressure of (a) 0, (b) 1.09, and (c) 1.52 GPa. The spectra at each temperature are shifted vertically. (d) Temperature and pressure dependence of ν_Q of CeCoSi and that of LaCoSi at ambient pressure. The vertical arrows indicate T_0 determined by NMR measurements, which detected it even at ambient pressure. The dashed line for LaCoSi indicates the conventional temperature dependence of ν_Q .

the magnetic ordering of Ce $4f$ moments, the only explanation for the NQR result is a cancellation of the internal magnetic field at the Co site, which is surrounded by four Ce ions. The transition to the underlying AFM state at T_N is of second-order, and this AFM state with $\mathbf{q} = \mathbf{0}$ does not break the translational symmetry of the crystal above T_0 . Then, the intermediate ordered state in $T_N < T < T_0$ should maintain the same translational symmetry, that is, the propagation vector is $\mathbf{q} = \mathbf{0}$. For the $\mathbf{q} = \mathbf{0}$ structure, the internal field is canceled only when the staggered Ce moment is along the $[001]$ axis [13]. This possibility is excluded by the increase of the susceptibility along this axis below T_0 [11]. Thus, we concluded that the ordered phase below T_0 is nonmagnetic with one tetragonal Co site. The unusual field response explained later also excludes the possibility of the magnetic state and yet indicates that this phase is not a simple paramagnetic state.

The temperature dependence of ν_Q usually obeys a conventional monotonous behavior $\nu_Q(T) =$

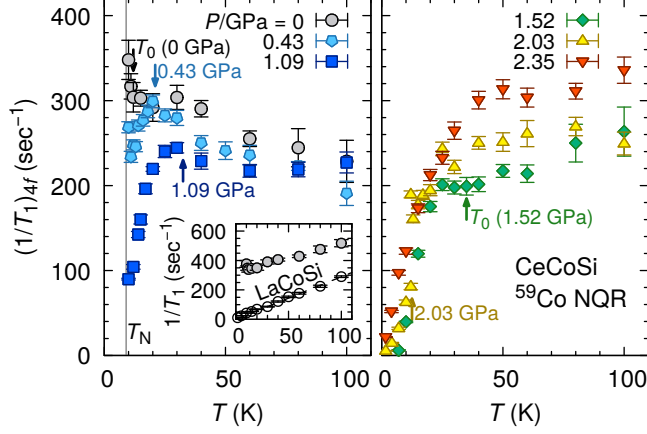


FIG. 2. (Color online) Temperature dependence of ^{59}Co NQR nuclear spin-lattice relaxation rate $1/T_1$ of CeCoSi from the Ce-4*f* electrons at $H = 0$ under several pressures. The 4*f* part was obtained by subtracting the $1/T_1$ value of LaCoSi. The vertical arrows indicate T_0 determined by NMR results. Inset (left panel): $1/T_1$ of CeCoSi at ambient pressure before subtraction as well as that of LaCoSi. The dashed line for LaCoSi shows the Korringa relation $1/T_1 \propto T$ in the normal metal.

$\nu_Q(0)(1 - \alpha T^{1.5})$ [14] ($\alpha > 0$) owing to the lattice expansion and vibration, as observed in LaCoSi. In contrast, the $\nu_Q(T)$ in CeCoSi deviates from this behavior above T_0 , and the deviation becomes remarkable as the pressure increases. Such behavior has been observed in some 4*f*-electron systems [15–19] and discussed to originate from a CEF splitting, a valence change of the 4*f* ion, or the Kondo effect. The distinct pressure dependence in CeCoSi indicates that such multiple effects influence ν_Q at the Co site through the pressure-enhanced hybridization between the 4*f* electron and conduction electrons.

Figure 2 shows the Ce-4*f* part of the nuclear spin-lattice relaxation rate $1/T_1$ measured by the NQR at $H = 0$. The $1/T_1$ has a Co 3*d* component, and it was subtracted using the result of LaCoSi (see the inset of the left panel of Fig. 2). The $1/T_1$ divided by temperature is shown in Supplemental Materials [13]. The $1/T_1$ of LaCoSi shows the weakly-correlated Pauli paramagnet corresponding to a previous report [20]. The absence of phase transition in LaCoSi is consistent with the interpretation that the phase below T_0 originates from Ce 4*f* electrons. No divergent behavior was detected near T_0 in $1/T_1$ in CeCoSi, indicating the absence of the magnetic critical fluctuations. A clear drop was found at T_0 only at 2.03 GPa. This may correspond to the gaplike anomaly in the electric resistivity above ~ 1.5 GPa [10] and suggest the decrease of the density of states. Around T_N , $1/T_1$ is expected to detect the magnetic fluctuations perpendicular to the [001]

axis [13]. $1/T_1$ diverged owing to the critical slowing down of the magnetic fluctuations at ambient pressure (see also Fig. 7 in the Supplemental Materials [13]). However, the divergence of $1/T_1$ is suppressed with increasing pressure. This is not expected with the magnetic structure of $\mathbf{m} \parallel [100]$. Two possibilities are considered to interpret this result. One is that the magnetic moment is tilted along the [001] axis under pressure. Another is that the magnetic fluctuation is suppressed as the ordered state below T_0 gets stabilized. The $1/T_1$ significantly above T_0 shows the localized Ce $4f$ electrons ($1/T_1 = \text{const.}$) at 1.52 GPa or below. Meanwhile, $1/T_1$ starts to decrease from higher temperatures than T_0 at 2.03 and 2.35 GPa. Such an itinerant behavior owing to coherent Kondo effect in $1/T_1$ is also seen in some heavy-fermion systems including CeCu_2Si_2 [21, 22]. The $1/T_1$ result, combined with the ν_Q behavior, indicate an enhancement of the Kondo effect by pressure.

Further information on the ordered state is provided by the spectra measured under a magnetic field. Figure 3(a) shows the full set of the NMR lines at ambient pressure at 10 K below $T_0 = 12$ K with a field strength of $\mu_0 H = 1.0$ T in addition to the results of 20 K. Here, $\theta = 87.8^\circ$ and 90° are the field angles from the [001] to [100] axes. At 20 K, seven NMR lines were observed owing to the nuclear quadrupole interaction of $I = 7/2$ ^{59}Co nucleus. Meanwhile, at 10 K, the third satellite at the lowest frequency split when the field was tilted from the [100] axis, clearly indicating the symmetry reduction below T_0 . The two-split peaks merged just when $H \parallel [100]$, which was consistent with the NQR data and suggesting that the crystallographic Co site remains one site below T_0 . Similar split and merging of the spectra were observed when the magnetic field is around [001] axis (not shown).

Figures 3(b)–3(d) show the temperature dependence of the NMR third satellite line with the field of $\mu_0 H = 1.0$ T slightly tilted from the [100] axis under pressures of 0, 1.09, and 1.52 GPa. The results under other pressures are shown in Supplemental Materials [13]. The spectra started to split at T_0 at all pressures, and the value of T_0 corresponds with the previous reports [11, 12]. This is the first microscopic evidence for the phase transition at T_0 at ambient pressure. Careful measurements just below T_0 , especially at ambient pressure, indicate that the transition is of second-order [13]. Three peaks were observed at intermediate temperatures at 1.52 GPa and other pressures [13], although it is unclear whether this is intrinsic or not. Here we assume the two-peak structure to be intrinsic because it is also observed at ambient pressure, where the stress or inhomogeneity owing to pressure is free.

The NMR line split is remarkable at the low-frequency third satellite line and disappears for $H \parallel [100]$. This situation is reproduced only when the induced magnetic field \mathbf{H}_{ind} is perpendicular

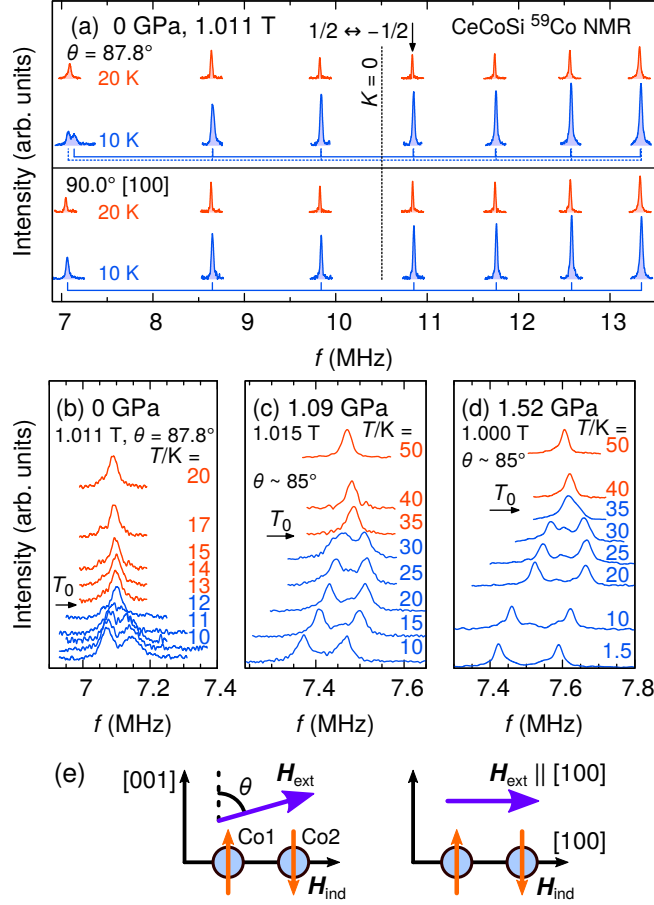


FIG. 3. (Color online) (a) ^{59}Co NMR spectra of CeCoSi at ambient pressure at 10 and 20 K with the field $\mu_0 H = 1.011$ T and angles $\theta = 87.8^\circ$ and 90° . The blue solid and dashed lines indicate the simulated peak frequencies at $T = 10$ K assuming the staggered field of $\sim \pm 15$ mT along the $[001]$ axis. The vertical arrow indicates the central ($1/2 \leftrightarrow -1/2$) line, whereas the vertical black dashed line indicates the frequency of $K = 0$ of the central line. (b–d) Temperature dependence of the spectra under pressures of (b) 0, (c) 1.09, and (d) 1.52 GPa with $\mu_0 H = 1.0$ T slightly tilted from the $[100]$ axis. The spectra are shifted vertically with an offset proportional to the temperatures. The horizontal arrows indicate T_0 . (e) Schematic of the induced field \mathbf{H}_{ind} under the external field \mathbf{H}_{ext} at the Co sites below T_0 . Only the $[001]$ components of \mathbf{H}_{ind} are drawn for simplicity.

to the external field, as shown in Fig. 3(e). The blue solid and dashed lines in Fig. 3(a) indicate the simulated NMR frequencies, where $\mu_0 H_{\text{ind},c} \sim \pm 15$ mT along the $[001]$ axis are adopted. When the external field \mathbf{H}_{ext} is tilted from $[100]$ to the $[001]$ axis, the total field at two Co sites, $\mathbf{H}_{\text{ext}} + \mathbf{H}_{\text{ind}}$, differs from each other, leading to the splitting of the NMR frequency. The field $\mu_0 H_{\text{ind},z} \sim \pm 15$ mT is absent in the NQR spectra, and thus, this is induced by the external field. Such an induced

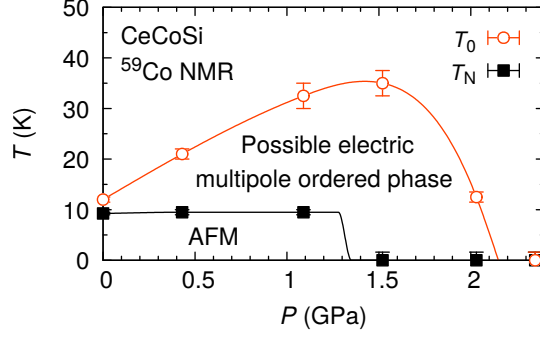


FIG. 4. (Color online) Temperature–pressure phase diagram of CeCoSi determined by the NMR and NQR results. The solid lines are guides to the eye. The transitions are of second-order across T_0 and T_N . The disappearing pressures of two phases are from Ref. 10.

field cannot be explained by a simple paramagnetic response of Ce $4f$ magnetic moment [13]. Notably, this excludes the possibility that the internal field at the Co site is canceled out in the AFM alignment of the Ce moments because tilting of the AFM moments under an external field yields a similar response to the paramagnetic response without splitting of the NMR line.

Figure 4 shows the temperature–pressure phase diagram of CeCoSi determined by our NMR and NQR results. The phase transition at T_0 at ambient pressure was unambiguously confirmed to be intrinsic from the microscopic point of view. Our results clearly demonstrate that second-order transitions occur successively across T_0 and T_N . The pressure dependence of T_0 is reminiscent of the Doniach-type phase diagram, implying that the c – f hybridization assists the stabilization of the ordered state at lower pressures. Two ordered phases are suppressed with increasing pressure, accompanied by the development of the Kondo effect, and the nonmagnetic ground state is realized in the pressure range of 1.4–2.15 GPa.

Our NMR and NQR results limit possible order parameters in CeCoSi as follows: in $T_N < T < T_0$, they exclude magnetically ordered states arising from Ce- $4f$ and Co- $3d$ electrons. Nonmagnetic ordered states arising from Co- $3d$ electrons, such as a charge density wave (CDW) or orbital ordering are also unlikely. If the CDW transition occurs, the spectra will be split into several sites corresponding to the superlattice formation. Similarly, if the phase transition lifts the Co- $3d$ orbital degeneracy protected by local tetragonal symmetry, orthorhombic transition is essential similar to an electronic nematic state in Fe pnictide systems[23]. The on-site NMR and NQR results did not show the corresponding symmetry reduction. As an ordered state of nonmagnetic Ce origin, the “metaorbital” transition [24], across which the occupancy of the Ce- $4f$ electrons changes steeply,

is proposed [10]; however, it does not correspond with the second-order transition with a symmetry reduction. The remaining possibility that should be considered is the contribution of electric degrees of freedom of Ce $4f$ electrons; that is, an electric multipole ordering. The CEF ground state of tetragonal CeCoSi is a Kramers doublet, but the AFQ ordering is possible if the state including the first-excited level possesses a large interlevel interaction [25], which is most likely enhanced by the Kondo effect. Quadrupolar degrees of freedom involving CEF excited states are also known in PrOs₄Sb₁₂ [26, 27] and CeTe [28].

Before deepening this discussion, we provide a general symmetry consideration, as discussed for the hidden-order state in URu₂Si₂ [29, 30]. Because the transition to the nonmagnetic state across T_0 in CeCoSi is second-order, the space group below T_0 must be one of the subgroups of the room-temperature phase of No. 129 ($P4/nmm$). Moreover, the underlying AFM state orders to $\mathbf{q} = \mathbf{0}$ structure, preserving the translational symmetry [8] while excluding the possibility of superlattice formation above T_N . Thus, the possible maximal subgroups are as follows: No. 59 ($Pm\bar{m}n$), 85 ($P4/n$), 90 ($P4_212$), 99 ($P4mm$), 113 ($P\bar{4}2_1m$), and 115 ($P\bar{4}m2$) [13, 31]. Because the Co site remains one site below T_0 , the space group with two Co sites, namely, No. 115, is unlikely. The breaking of the four-fold symmetry was not detected at the Co site, which contradicts No. 59, 90, and 99 with two-fold symmetry at the Co site. Therefore, the space group No. 85 or No. 113 is preferable for the state below T_0 in CeCoSi. An interesting feature is that the symmetry reduction to No. 85 or No. 113 does not require the shift of the atomic positions [13, 31], that is, it can be satisfied by symmetrical change of electronic configurations of the Ce ions. If that is the case, the lattice distortion is triggered by the weak coupling to the electrons, and the detection of the symmetry change may not be straightforward in X-ray measurements. This would happen in URu₂Si₂ [29, 30]. Moreover, the No. 113 lacks global inversion symmetry; therefore, experimental methods that can observe the splitting of bands will be effective to confirm this.

A clue to understand the origin of this phase is the unusual field response, i.e., the induced field perpendicular to the external field. Such a behavior is reminiscent of an AFQ state [32, 33], as observed in ferro- or antiferroquadrupolar systems CeB₆ [34], PrFe₄P₁₂ [35, 36], PrTi₂Al₂₀ [37], and NpO₂ [38]. Therefore, it is reasonable to consider the ordered state in CeCoSi as an AFQ state. Along this line of thought, a crucial point is consistency between the experiment and theoretical suggestion [25]. In the case of multipolar states, the space groups No. 85 and 113, suggested by the NQR result, correspond to the hexadecapolar and O_{xy} -type AFQ states, respectively. The symmetry of the Ce site reduces to four-fold symmetry without mirror operations (4..) in the

No. 85 and two-fold symmetry ($2.mm$) in the No. 113 space group [13]. Meanwhile, identification of the AFQ order parameter is possible in principle from the NMR-line splitting by a theoretical work[39]. For example, the NMR line can split in the O_{zx} -type AFQ state when $H \perp [010]$, except for $H \parallel [100]$ and $H \parallel [001]$. Therefore, the induced field detected by our NMR suggests the O_{zx} -type AFQ state. In the case of O_{xy} type, which is proposed by the zero-field result, the line splitting does not occur by the component along $[001]$ of the field. Thus, we need to resolve this discrepancy between zero- and finite-field results to settle the origin of the ordered state. A point to be considered is the switching of the order parameter under field, as in some quadrupole systems such as CeB_6 [40] and $\text{PrTi}_2\text{Al}_{20}$ [41]. Such a signature has not been observed thus far in CeCoSi , but investigations for the field-induced switching may unravel this issue. Another point is the lack of local inversion symmetry at the Ce site. In this case, odd-parity multipoles, such as electric octapole, are active in principle through the antisymmetric spin-orbit interaction at the Ce site, but the mechanism through which this effect influences the field response is unknown. In any case, our results capturing a peculiarity of the ordered state in CeCoSi will offer theoretical and further experimental challenges for the complete elucidation of the order parameter.

In conclusion, we have performed single-crystalline NMR and NQR measurements to investigate the unresolved ordered state in CeCoSi . The absence of any signature of symmetry reduction in the ^{59}Co -NQR spectra indicates that the ordered phase below T_0 is nonmagnetic and originates from Ce $4f$ electrons. An unusual field response, proved by the NMR-line splitting, characterizes the extraordinary ordered state, indicating that it is most likely the electric multipole state. Our results show that CeCoSi undergoes two types of second-order phase transitions with different symmetry lowerings, and the nonmagnetic phase can be the ground state above ~ 1.4 GPa. It is interesting to consider why CeCoSi differs from other non-cubic systems. As an idea, we expect that parity mixing by absence of the local inversion symmetry at the Ce site may be a key factor to induce this peculiar behavior in CeCoSi . In any case, CeCoSi is a novel example offering profound physics originating from the $4f^1$ state.

The authors thank M. Yatsushiro, S. Hayami, H. Hidaka, Y. Tokunaga, K. Ishida, and Y. Kuramoto for their insightful discussions. This work was supported by a Grant-in-Aid for Scientific Research on Innovative Areas “J-Physics” (Grants No. 15H05882, No. 15H05885, No. JP18H04320, and No. JP18H04321), and a Grant-in-Aid for JSPS Research Fellow (Grant No. JP19J00336) from JSPS.

* manago@riko.shimane-u.ac.jp; Present address: Department of Physics and Materials Science, Graduate School of Natural Science and Technology, Shimane University, Matsue, Shimane, Japan.

- [1] J. A. Mydosh and P. M. Oppeneer, *Rev. Mod. Phys.* **83**, 1301 (2011).
- [2] J. A. Mydosh, P. M. Oppeneer, and P. S. Riseborough, *J. Phys.: Condens. Matter* **32**, 143002 (2020).
- [3] R. Okazaki, T. Shibauchi, H. J. Shi, Y. Haga, T. D. Matsuda, E. Yamamoto, Y. Onuki, H. Ikeda, and Y. Matsuda, *Science* **331**, 439 (2011).
- [4] C. Tabata, T. Inami, S. Michimura, M. Yokoyama, H. Hidaka, T. Yanagisawa, and H. Amitsuka, *Philos. Mag.* **94**, 3691 (2014).
- [5] S. C. Riggs, M. Shapiro, A. V. Maharaj, S. Raghu, E. Bauer, R. Baumbach, P. Giraldo-Gallo, M. Wartenbe, and I. Fisher, *Nat. Commun.* **6**, 6425 (2015).
- [6] L. Wang, M. He, F. Hardy, D. Aoki, K. Willa, J. Flouquet, and C. Meingast, *Phys. Rev. Lett.* **124**, 257601 (2020).
- [7] O. I. Bodak, E. I. Gladyshevskii, and P. I. Kripyakevich, *J. Struct. Chem.* **11**, 283 (1970).
- [8] S. E. Nikitin, D. G. Franco, J. Kwon, R. Bewley, A. Podlesnyak, A. Hoser, M. M. Koza, C. Geibel, and O. Stockert, *Phys. Rev. B* **101**, 214426 (2020).
- [9] B. Chevalier and S. F. Matar, *Phys. Rev. B* **70**, 174408 (2004).
- [10] E. Lengyel, M. Nicklas, N. Caroca-Canales, and C. Geibel, *Phys. Rev. B* **88**, 155137 (2013).
- [11] H. Tanida, K. Mitsumoto, Y. Muro, T. Fukuhara, Y. Kawamura, A. Kondo, K. Kindo, Y. Matsumoto, T. Namiki, T. Kuwai, and T. Matsumura, *J. Phys. Soc. Jpn.* **88**, 054716 (2019).
- [12] H. Tanida, Y. Muro, and T. Matsumura, *J. Phys. Soc. Jpn.* **87**, 023705 (2018).
- [13] (Supplemental Materials) It contains the NMR Knight shift, hyperfine coupling, examination of the breaking of the four-fold symmetry, temperature evolution of the NMR line split, NMR and NQR spectra not shown in the main text, NQR spectra at the AFM state, nuclear spin-lattice relaxation rate divided by temperature $1/T_1T$, and the details of the possible space groups below T_0 .
- [14] J. Christiansen, P. Heubes, R. Keitel, W. Klinger, W. Loeffler, W. Sandner, and W. Witthuhn, *Z. Phys. B* **24**, 177 (1976).
- [15] T. Shimizu, H. Yasuoka, Z. Fisk, and J. L. Smith, *J. Phys. Soc. Jpn.* **56**, 4113 (1987).
- [16] S. Kitagawa, T. Higuchi, M. Manago, T. Yamanaka, K. Ishida, H. S. Jeevan, and C. Geibel, *Phys. Rev. B* **96**, 134506 (2017).

- [17] T. Mito, H. Hara, T. Ishida, K. Nakagawara, T. Koyama, K. Ueda, T. Kohara, K. Ishida, K. Matsubayashi, Y. Saiga, and Y. Uwatoko, *J. Phys. Soc. Jpn.* **82**, 103704 (2013).
- [18] K.-i. Magishi, H. Sugawara, M. Takahashi, T. Saito, K. Koyama, T. Saito, S. Tatsuoka, K. Tanaka, and H. Sato, *J. Phys. Soc. Jpn.* **81**, 124706 (2012).
- [19] M. Yogi, H. Niki, T. Kawata, and C. Sekine, *JPS Conf. Proc.* **81**, 011046 (2014).
- [20] R. Welter, G. Venturini, E. Ressouche, and B. Malaman, *J. Alloys Compd.* **210**, 279 (1994).
- [21] K. Ishida, Y. Kawasaki, K. Tabuchi, K. Kashima, Y. Kitaoka, K. Asayama, C. Geibel, and F. Steglich, *Phys. Rev. Lett.* **82**, 5353 (1999).
- [22] K. Fujiwara, Y. Hata, K. Kobayashi, K. Miyoshi, J. Takeuchi, Y. Shimaoka, H. Kotegawa, T. C. Kobayashi, C. Geibel, and F. Steglich, *J. Phys. Soc. Jpn.* **77**, 123711 (2008).
- [23] S. Kasahara, H. J. Shi, K. Hashimoto, S. Tonegawa, Y. Mizukami, T. Shibauchi, K. Sugimoto, T. Fukuda, T. Terashima, A. H. Nevidomskyy, and Y. Matsuda, *Nature (London)* **486**, 382 (2012).
- [24] K. Hattori, *J. Phys. Soc. Jpn.* **79**, 114717 (2010).
- [25] M. Yatsushiro and S. Hayami, *J. Phys. Soc. Jpn.* **89**, 013703 (2020).
- [26] M. Kohgi, K. Iwasa, M. Nakajima, N. Metoki, S. Araki, N. Bernhoeft, J.-M. Mignot, A. Gukasov, H. Sato, Y. Aoki, and H. Sugawara, *J. Phys. Soc. Jpn.* **72**, 1002 (2003).
- [27] T. Goto, Y. Nemoto, K. Sakai, T. Yamaguchi, M. Akatsu, T. Yanagisawa, H. Hazama, K. Onuki, H. Sugawara, and H. Sato, *Phys. Rev. B* **69**, 180511 (2004).
- [28] Y. Kawarasaki, T. Matsumura, M. Sera, and A. Ochiai, *J. Phys. Soc. Jpn.* **80**, 023713 (2011).
- [29] H. Harima, K. Miyake, and J. Flouquet, *J. Phys. Soc. Jpn.* **79**, 033705 (2010).
- [30] S. Kambe, Y. Tokunaga, H. Sakai, T. Hattori, N. Higa, T. D. Matsuda, Y. Haga, R. E. Walstedt, and H. Harima, *Phys. Rev. B* **97**, 235142 (2018).
- [31] T. Hahn, ed., *International tables for crystallography*, 5th ed., Vol. A (Springer, 2005) corrected reprint of the 5th edition.
- [32] R. Shiina, H. Shiba, and P. Thalmeier, *J. Phys. Soc. Jpn.* **66**, 1741 (1997).
- [33] O. Sakai, R. Shiina, H. Shiba, and P. Thalmeier, *J. Phys. Soc. Jpn.* **66**, 3005 (1997).
- [34] M. Takigawa, H. Yasuoka, T. Tanaka, and Y. Ishizawa, *J. Phys. Soc. Jpn.* **52**, 728 (1983).
- [35] K. Ishida, H. Murakawa, K. Kitagawa, Y. Ihara, H. Kotegawa, M. Yogi, Y. Kitaoka, B.-L. Young, M. S. Rose, D. E. MacLaughlin, H. Sugawara, T. D. Matsuda, Y. Aoki, H. Sato, and H. Harima, *Phys. Rev. B* **71**, 024424 (2005).
- [36] J. Kikuchi, M. Takigawa, H. Sugawara, and H. Sato, *J. Phys. Soc. Jpn.* **76**, 043705 (2007).

- [37] T. Taniguchi, M. Yoshida, H. Takeda, M. Takigawa, M. Tsujimoto, A. Sakai, Y. Matsumoto, and S. Nakatsuji, *J. Phys. Soc. Jpn.* **85**, 113703 (2016).
- [38] Y. Tokunaga, Y. Homma, S. Kambe, D. Aoki, H. Sakai, E. Yamamoto, A. Nakamura, Y. Shiokawa, R. E. Walstedt, and H. Yasuoka, *Phys. Rev. Lett.* **94**, 137209 (2005).
- [39] M. Yatsushiro and S. Hayami, *Phys. Rev. B* **102**, 195147 (2020).
- [40] S. Nakamura, T. Goto, and S. Kunii, *J. Phys. Soc. Jpn.* **64**, 3941 (1995).
- [41] T. Taniguchi, K. Hattori, M. Yoshida, H. Takeda, S. Nakamura, T. Sakakibara, M. Tsujimoto, A. Sakai, Y. Matsumoto, S. Nakatsuji, and M. Takigawa, *J. Phys. Soc. Jpn.* **88**, 084707 (2019).

Supplemental Materials for
**“Unusual Nonmagnetic Ordered State in CeCoSi Revealed by ^{59}Co -NMR and
NQR Measurements”**

Masahiro Manago, Hisashi Kotegawa, Hideki Tou, and Hisatomo Harima
Department of Physics, Kobe University, Kobe, Hyogo 657-8501, Japan

Hiroshi Tanida
Liberal Arts and Sciences, Toyama Prefectural University, Imizu, Toyama 939-0398, Japan

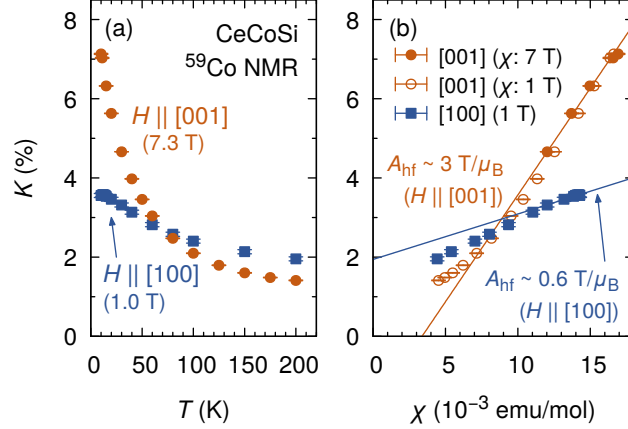


FIG. 1. (a) ^{59}Co NMR Knight shift in CeCoSi at ambient pressure with the field along the [100] (at 1 T) and [001] (at 7.3 T) directions above T_N . (b) The relation between χ and K with temperatures as an implicit parameter (K - χ plot). The susceptibility is from Ref. 1. For the [001] direction, the susceptibility results are shown for the 1 and 7 T. The hyperfine coupling constant A_{hf} was deduced from the linear fit of the K values against the χ below 30 K.

NMR KNIGHT SHIFT AT AMBIENT PRESSURE

When the magnetic field is applied to the system, the nucleus feels the internal field created by the electrons through the hyperfine interaction in addition to the applied field. This internal field is usually expressed as the dimensionless Knight shift tensor K , and the total magnetic field is $\mathbf{H}_{\text{tot}} = (1 + K)\mathbf{H}_0$, where the \mathbf{H}_0 represents the applied field. The form of the Knight shift tensor is restricted by the local symmetry of the nucleus. In the case of the Co site in the non-ordered state in CeCoSi, the Knight shift at the Co site is the form of

$$K = \begin{pmatrix} K_{aa} & 0 & 0 \\ 0 & K_{aa} & 0 \\ 0 & 0 & K_{cc} \end{pmatrix}, \quad (1)$$

where the c represent the [001] direction, because of the $\bar{4}m2$ local tetragonal symmetry. The measurements with $H \parallel [100]$ and [001] give the full information of the Knight shift tensor in the non-ordered state above T_0 .

Because the ^{59}Co nucleus ($I = 7/2$, nuclear gyromagnetic ratio $\gamma_n/2\pi = 10.03$ MHz/T, and electric quadrupole moment $Q = 0.42 \times 10^{-28}$ m² [2, 3]) interacts with the electric field gradient of the atomic site, the NMR spectra splits into seven ($2I$) lines. The value of the ^{59}Co Knight

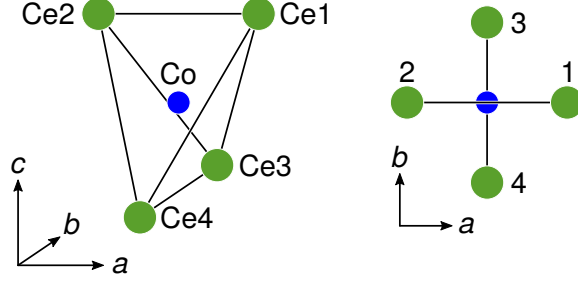


FIG. 2. Left: The Co atom and the four nearest Ce atoms forming a tetrahedron. The smaller and the larger balls indicate Co and Ce atoms, respectively. Right: Top view of the left panel. The Ce atoms do not locate at the same plane.

shift was extracted from the frequency of the central peak the seven quadrupole split spectra. The effect of the quadrupole shift was subtracted by numerical diagonalization of the total nuclear Hamiltonian. Figure 1(a) shows the ^{59}Co NMR Knight shift along the [100] and [001] directions in the single-crystalline CeCoSi sample at ambient pressure. The sample direction was aligned by eye, and the misalignment of the field is typically an order of $\sim 5^\circ$. The Knight shift increased as the temperature gets lower, as observed in the macroscopic susceptibility [1, 4]; however, contrary to the almost isotropic susceptibility, the Knight-shift value is about 2 times larger for [001] directions than that of [100] just above T_N . Figure 1(b) shows the relation between the susceptibility χ and the Knight shift K with the temperature as an implicit parameter (the K - χ plot). The susceptibility was referred from Ref. 1. The relation $K = A_{\text{hf}}\chi + K_0$ roughly holds for these directions. The kink in the K - χ plot is seen at 60–100 K depending on the directions, and it is probably due to the crystal electric field effect. The estimated hyperfine coupling constants are $A_{\text{hf}}^a \sim 0.6 \text{ T}/\mu_B$ for the [100] and $A_{\text{hf}}^c \sim 3 \text{ T}/\mu_B$ for the [001] direction. The experimental results below 30 K were used for analyzing A_{hf} values.

HYPERFINE COUPLING BETWEEN THE Co NUCLEUS AND $4f$ ELECTRONS

Here we present the symmetry consideration of the hyperfine coupling tensor of the Co site. The Co site is surrounded by four Ce atoms, which form a tetrahedron, as shown in Fig. 2. The internal field at the Co site created by these nearest Ce moments are written as

$$\mathbf{H}_{\text{int}} = \sum_{i=1}^4 \mathbf{B}_i \cdot \mathbf{m}_i, \quad (2)$$

where \mathbf{B}_i is the coupling tensor between i site and \mathbf{m}_i is the magnetic moment of the i site. The structure of \mathbf{B}_i and the relation between different i sites are restricted by the crystallographic symmetry. In the state above T_0 , the crystal structure is tetragonal $P4/nmm$, and the Co site is located at the $\bar{4}m2$ site. This leads to

$$\mathbf{B}_1 = \begin{pmatrix} B_{aa} & 0 & B_{ac} \\ 0 & B_{bb} & 0 \\ B_{ca} & 0 & B_{cc} \end{pmatrix} \quad (3)$$

for the site 1. Then, the site 2 in the same z plane as 1 satisfies

$$\mathbf{B}_2 = \begin{pmatrix} B_{aa} & 0 & -B_{ac} \\ 0 & B_{bb} & 0 \\ -B_{ca} & 0 & B_{cc} \end{pmatrix} \quad (4)$$

because the site 2 is connected to the site 1 through the C_2 rotation with respect to the z axis. The site 3 and 4 are connected to the site 1 and 2 through the S_4 operation, leading to

$$\mathbf{B}_3 = \begin{pmatrix} B_{bb} & 0 & 0 \\ 0 & B_{aa} & -B_{ac} \\ 0 & -B_{ca} & B_{cc} \end{pmatrix}, \quad \mathbf{B}_4 = \begin{pmatrix} B_{bb} & 0 & 0 \\ 0 & B_{aa} & B_{ac} \\ 0 & B_{ca} & B_{cc} \end{pmatrix}. \quad (5)$$

In the state above T_0 , all the Ce moments point to the same direction, and thus, the internal field at the Co site is

$$\mathbf{H}_{\text{int}} = (\mathbf{B}_1 + \mathbf{B}_2 + \mathbf{B}_3 + \mathbf{B}_4) \cdot \mathbf{m} \quad (6)$$

$$= \begin{pmatrix} 2(B_{aa} + B_{bb}) & 0 & 0 \\ 0 & 2(B_{aa} + B_{bb}) & 0 \\ 0 & 0 & 4B_{cc} \end{pmatrix} \cdot \mathbf{m} \quad (7)$$

$$\equiv \begin{pmatrix} A_{\text{hf}}^a & 0 & 0 \\ 0 & A_{\text{hf}}^a & 0 \\ 0 & 0 & A_{\text{hf}}^c \end{pmatrix} \cdot \mathbf{m}. \quad (8)$$

The microscopic hyperfine coupling constants B_{ij} are related to A_{hf}^a and A_{hf}^c introduced in the previous section.

If the $\mathbf{q} = \mathbf{0}$ AFM ordering occurs, the moments satisfies $\mathbf{m}_1 = \mathbf{m}_2 = -\mathbf{m}_3 = -\mathbf{m}_4 \equiv \mathbf{m}_{\text{AFM}}$, and

the internal field is

$$\mathbf{H}_{\text{int}} = (\mathbf{B}_1 + \mathbf{B}_2 - \mathbf{B}_3 - \mathbf{B}_4) \cdot \mathbf{m}_{\text{AFM}} \quad (9)$$

$$= \begin{pmatrix} 2(B_{aa} - B_{bb}) & 0 & 0 \\ 0 & -2(B_{aa} - B_{bb}) & 0 \\ 0 & 0 & 0 \end{pmatrix} \cdot \mathbf{m}_{\text{AFM}}. \quad (10)$$

The staggered component along the z axis is cancelled at the Co site, and especially, the internal field is absent when $\mathbf{m}_{\text{AFM}} \parallel [001]$. Therefore, it is unusual that the NMR line splits with an induced field along the $[001]$ direction below T_0 .

If the $\mathbf{q} = \mathbf{0}$ AFM causes orthorhombic distortion, the relation of \mathbf{B}_i between different Ce sites can be altered. For instance, the distortion along the $[100]$ direction breaks the relation between the pairs of (1,2) and (3,4) sites, leading

$$\mathbf{H}_{\text{int}} = (\mathbf{B}_1 + \mathbf{B}_2 - \mathbf{B}'_3 - \mathbf{B}'_4) \cdot \mathbf{m}_{\text{AFM}} \quad (11)$$

$$= \begin{pmatrix} 2(B_{aa} - B'_{bb}) & 0 & 0 \\ 0 & -2(B'_{aa} - B_{bb}) & 0 \\ 0 & 0 & 2(B_{cc} - B'_{cc}) \end{pmatrix} \cdot \mathbf{m}_{\text{AFM}}. \quad (12)$$

The internal field along the $[001]$ direction is possible if the staggered moments tilt from the $[001]$ plane.

If the AFM state is not limited to $\mathbf{q} = \mathbf{0}$, the internal field can emerge along the $[001]$ direction, although such a magnetic structure is inconsistent with the ordered state below T_0 . For instance, in the checkerboard structure with $\mathbf{q} = (\pi/a, \pi/a, 0)$ (a is the lattice constant), the moments satisfy $\mathbf{m}_1 = -\mathbf{m}_2 = \mathbf{m}_3 = -\mathbf{m}_4 \equiv \mathbf{m}_{\text{AFM}}$. The internal field is

$$\mathbf{H}_{\text{int}} = (\mathbf{B}_1 - \mathbf{B}_2 + \mathbf{B}_3 - \mathbf{B}_4) \cdot \mathbf{m}_{\text{AFM}} \quad (13)$$

$$= \begin{pmatrix} 0 & 0 & 2B_{ac} \\ 0 & 0 & 2B_{ac} \\ 2B_{ca} & 2B_{ca} & 0 \end{pmatrix} \cdot \mathbf{m}_{\text{AFM}}. \quad (14)$$

The internal field along the $[001]$ direction is induced when the \mathbf{m}_{AFM} lies in the plane.

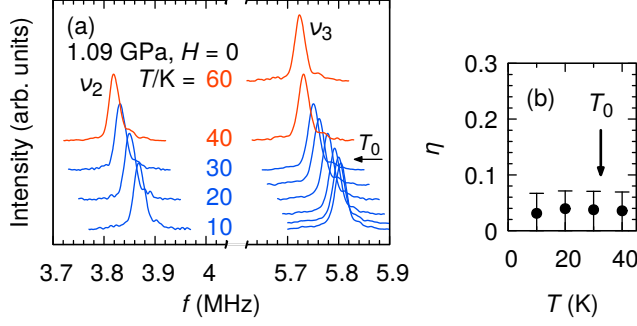


FIG. 3. (a) ^{59}Co NQR spectra without a field at 1.09 GPa in CeCoSi. (b) The temperature dependence of the asymmetric parameter η at 1.09 GPa deduced from the NQR frequencies shown in (a).

EXAMINATION OF THE TETRAGONAL SYMMETRY BELOW T_0 BY NQR

We examined whether the tetragonal symmetry at the Co site is preserved below T_0 or not using the ^{59}Co NQR spectra. The nuclear-spin Hamiltonian without the magnetic field is

$$\mathcal{H}_Q = \frac{\hbar\omega_Q}{6} \left\{ [3I_z^2 - I(I+1)] + \frac{1}{2}\eta(I_+^2 + I_-^2) \right\}, \quad (15)$$

where ω_Q is the quadrupole frequency, η is the asymmetric parameter. The coordinate in the above equation is chosen so that the electronic field gradient at the nuclear site (V_{ij}) is diagonalized and satisfies the relation $|V_{zz}| \geq |V_{yy}| \geq |V_{xx}|$. The ω_Q is proportional to V_{zz} along the [001] axis (the maximum principal axis), and the asymmetric parameter is $\eta = |V_{xx} - V_{yy}|/|V_{zz}|$ and satisfies $0 \leq \eta \leq 1$.

In the case of the ^{59}Co ($I = 7/2$) site in CeCoSi above T_0 , $\eta = 0$ by the local symmetry $\bar{4}m2$ ($\bar{4}$ is the sufficient condition for $\eta = 0$) and the z axis is the [001] direction. Then, the three NQR lines arise from the $\pm m \leftrightarrow \pm(m+1)$ ($m = 1/2, 3/2, \text{ and } 5/2$) level transitions with the resonant frequencies $\nu_i = i\nu_Q$ ($i \equiv m + 1/2 = 1, 2, 3$), where $\nu_Q \equiv \omega_Q/(2\pi)$.

If the $\bar{4}$ symmetry of the Co is lost below T_0 , η gets a nonzero value, and the frequency ν_i no longer has an integer ratio. Within the second-order perturbation theory with respect to the η term, the ratio between ν_2 and ν_3 for the $I = 7/2$ nuclei is

$$\frac{\nu_3}{\nu_2} = \frac{3}{2} + \frac{7}{10}\eta^2. \quad (16)$$

Thus, measurements of the (at least) two NQR lines enable us to examine whether the tetragonal symmetry is broken or not at the Co site. NMR spectra with a magnetic field is more sensitive to the emergence of a small η in general; however, we chose the NQR spectra to find η this time because

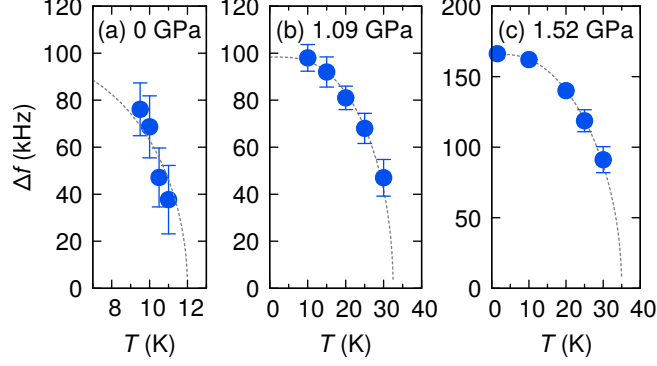


FIG. 4. (a–c) Temperature dependence of the split width Δf of the ^{59}Co NMR lines below T_0 at (a) 0, (b) 1.09, and (c) 1.52 GPa. The dashed lines indicate the temperature evolution of the BCS-type order parameter. Parameters of the curve at 0 GPa were given by hand, while the results at 1.09 and 1.52 GPa were obtained by a least-square method.

anomalous splitting occurs with applying field below T_0 in NMR, which makes the deduction of η difficult.

Figure 3(a) shows the part of the ^{59}Co NQR spectra at the ν_2 and ν_3 lines at 1.09 GPa. The obtained asymmetric parameter η is shown in Fig. 3(b). The value of η remains almost zero below $T_0 \simeq 33$ K, meaning that the breaking of the tetragonal symmetry at the Co site was not detected by the NQR spectra. Although we cannot exclude the possibility that the tetragonal symmetry is broken with a nonzero η below the detection limit, it is more likely that CeCoSi remains tetragonal because the phase transition at T_0 was clearly detected in the ν_Q .

ANALYSIS OF THE NMR SPLIT DISTANCE

Figures 4(a–c) show the temperature dependence of the NMR split distance at 0, 1.09, and 1.52 GPa. The distance Δf , or the difference of the two peaks in frequency, monotonically increases below T_0 . These results are consistent with the second-order transition. We tentatively adopt the BCS-type temperature evolution of the order parameter to reproduce Δf assuming that it is proportional to the order parameter. We used an approximate function of the order parameter to reproduce the experiments:

$$\Delta f(T) = \Delta f_0 \tanh \left[a(T_c/T - 1)^{1/2} \right], \quad (17)$$

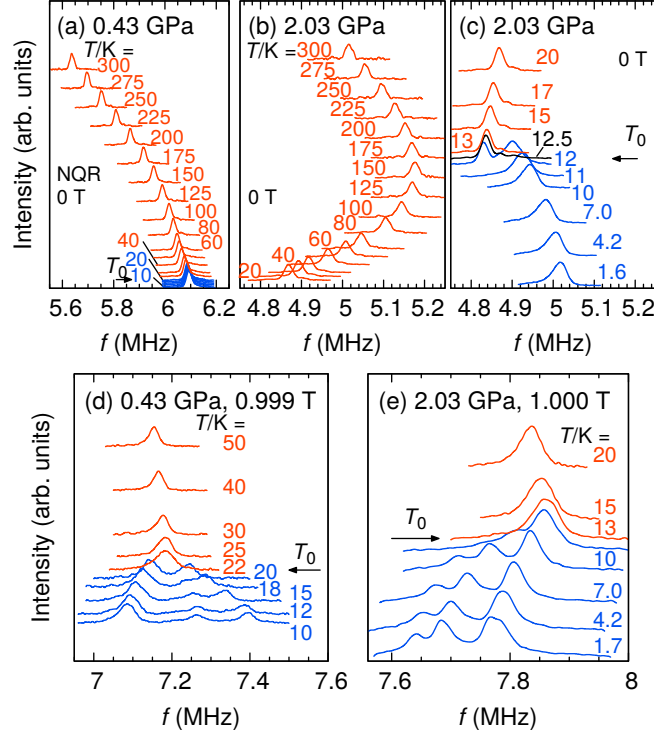


FIG. 5. (a–c) ^{59}Co NQR spectra without an external field at (a) 0.43 and (b,c) 2.03 GPa in CeCoSi. (d,e) The NMR spectra at (d) 0.43 and (e) 2.03 GPa under the field of $\mu_0 H = 1$ T. The field angle was $\theta \sim 85^\circ$ at these pressures.

where Δf_0 and a are fitting parameters. The results are shown with the dashed lines. The theoretical curves were roughly in agreement with the experiments.

NMR AND NQR SPECTRA AT 0.43 AND 2.03 GPa

Figures 5(a–c) show the NQR spectra at 0.43 and 2.03 GPa. The kink is clearer at 2.03 GPa than at 0.43 GPa, and the $\nu_Q(T)$ gets a maximum at 2.03 GPa.

Figures 5(d,e) show the NMR spectra at 0.43 and 2.03 GPa under the field of 1 T with the angle $\theta \sim 85^\circ$. The spectra started to split at T_0 in these pressures, indicating the symmetry reduction. The number of peaks is three in these cases. We performed measurements in the order of 1.09, 1.52, 2.03, and 0.43 GPa. Three peaks were remarkably observed in the last two pressures. We suspect the possibility that the sample may be damaged by the successive application of pressure. It is a future task to confirm whether more than two peaks is an intrinsic phenomenon or not.

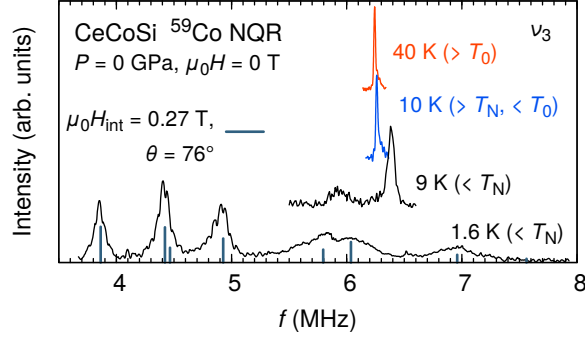


FIG. 6. ^{59}Co NQR spectra without an external field at ambient pressure in several temperatures in CeCoSi. The spectra are shifted vertically. The vertical lines for the result at 1.6 K are the calculated result with the internal field of 0.27 T and the angle 76° from the [001] axis.

NQR SPECTRA IN THE ANTIFERROMAGNETIC STATE

We measured the NQR (zero-field NMR) spectrum in the antiferromagnetic (AFM) state at ambient pressure to get information about the magnetic structure. Figure 6 shows the spectra at 9 and 1.6 K below T_N at ambient pressure in addition to the results above T_N . The NQR spectrum started to split at 9 K and showed a complicated structure with many peaks because of the internal field in the AFM state. The simulated spectra are shown with vertical lines in Fig. 6. The best fit of the experiments was obtained with the internal field $\mu_0 H_{\text{int}} = 0.27$ T and the field angle $\theta = 76^\circ$ from the [001] axis at the Co site. The Co site remains one site below T_N . This result indicates the commensurate AFM structure, and is consistent with the polarized neutron scattering measurement [5]. Although the neutron experiment indicates that the Ce moment is parallel to the [100] direction, our data suggests that the Ce moments slightly tilt to the [001] direction, which makes the $\theta < 90^\circ$, i.e., the emergence of the internal field along the [001] direction at the Co site. This is possible because of the orthorhombic distortion of the crystal, as mentioned above. The tilt of the Ce moment is consistent with the susceptibility drop at T_N in the [001] direction as well as in the [100] [1].

NUCLEAR SPIN-LATTICE RELAXATION RATE $1/T_1$

Figure 7 shows the ^{59}Co nuclear spin-lattice relaxation rate $1/T_1$ divided by temperature $1/T_1 T$ in CeCoSi. The Co 3d part was subtracted using the results of LaCoSi. $1/T_1$ can detect the magnetic

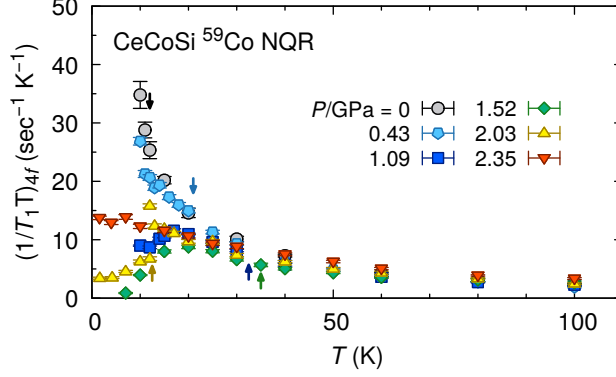


FIG. 7. Temperature dependence of ^{59}Co NQR nuclear spin-lattice relaxation rate divided by temperature $1/T_1T$ of CeCoSi from the Ce-4*f* electrons. The vertical arrows indicate T_0 .

fluctuations perpendicular to the maximum principal axis of the electric field gradient ([001] axis in the Co site). $1/T_1T$ increases as the temperature decreases much above T_0 in any pressure, reflecting the localized nature of the 4*f* electrons. $1/T_1T$ showed a critical magnetic fluctuations around T_N at ambient pressure. However, the divergence of $1/T_1T$ was suppressed at 1.09 GPa. The stabilization of the ordered phase below T_0 may be related to this suppression, as discussed in the main text.

LIST OF POSSIBLE SPACE GROUPS BELOW T_0

Details of the possible space groups below T_0 are shown in Tab. I [6]. The maximal subgroups of the No. 129 ($P4/nmm$) without superstructure are chosen. The No. 129 is a primitive tetragonal group, and 16 symmetry operations belong to this group. In the maximal subgroups, 8 symmetry operations remain. There is an orthorhombic space group (No. 59), and the others are tetragonal. Because the unit cell volume does not change across the transition for these groups, the multiplicity of the atom should be preserved. In some space groups, Ce or Co sites split into two inequivalent sites. The No. 85 and No. 113 are consistent with our NQR results, as discussed in the main text. The atomic positions do not need to shift, i.e., the notation of the coordinate remains unchanged, across the transition to the space groups No. 85 and No. 113.

TABLE I. Possible space groups for the ordered state below T_0 in CeCoSi. The Wyckoff letter and the site symmetry of the atoms are shown for each space group. The atomic position is shown when the notation changes or the atomic position splits. The first row shows the space group No. 129 in the room-temperature state in the origin choice 1. The apparent shift of the positions in No. 99 is due to the change of the origin.

Space group	Ce site	Co site	Si site
No. 129 $P4/nmm$	$2c$ $4mm$ $(0, 1/2, z)$, $(1/2, 0, \bar{z})$	$2a$ $\bar{4}m2$ $(0, 0, 0)$, $(1/2, 1/2, 0)$	$2c$ $4mm$ $(0, 1/2, z)$, $(1/2, 0, \bar{z})$
No. 59 $Pmmm$	$2a$ $mm2$	$2b$ $mm2$	$2a$ $mm2$
No. 85 $P4/n$	$2c$ $4..$	$2a$ $\bar{4}..$	$2c$ $4..$
No. 90 $P42_12$	$2c$ $4..$	$2a$ 2.22	$2c$ $4..$
No. 99 $P4mm$	$1a$ $4mm$ $(0, 0, z)$; $1b$ $4mm$ $(1/2, 1/2, z')$	$2c$ $2mm.$ $(1/2, 0, z)$, $(0, 1/2, z)$	$1a$ $4mm$ $(0, 0, z)$; $1b$ $4mm$ $(1/2, 1/2, z')$
No. 113 $P\bar{4}2_1m$	$2c$ $2.mm$	$2a$ $\bar{4}..$	$2c$ $2.mm$
No. 115 $P\bar{4}m2$	$2g$ $2mm.$	$1a$ $\bar{4}m2$ $(0, 0, 0)$; $1b$ $\bar{4}m2$ $(1/2, 1/2, 0)$	$2g$ $2mm.$

- [1] H. Tanida, K. Mitsumoto, Y. Muro, T. Fukuhara, Y. Kawamura, A. Kondo, K. Kindo, Y. Matsumoto, T. Namiki, T. Kuwai, and T. Matsumura, Successive phase transition at ambient pressure in CeCoSi: Single crystal studies, *J. Phys. Soc. Jpn.* **88**, 054716 (2019).
- [2] G. C. Carter, L. H. Bennett, and D. J. Kahan, *Metallic Shifts in NMR* (Pergamon press, New York, 1977).
- [3] J. R. de Laeter, J. K. Böhlke, P. De Bièvre, H. Hidaka, H. S. Peiser, K. J. R. Rosman, and P. D. P. Taylor, Atomic weights of the elements. review 2000 (iupac technical report), *Pure Appl. Chem.* **75**, 683 (2003).
- [4] E. Lengyel, M. Nicklas, N. Caroca-Canales, and C. Geibel, Temperature-pressure phase diagram of CeCoSi: Pressure-induced high-temperature phase, *Phys. Rev. B* **88**, 155137 (2013).
- [5] S. E. Nikitin, D. G. Franco, J. Kwon, R. Bewley, A. Podlesnyak, A. Hoser, M. M. Koza, C. Geibel, and O. Stockert, Gradual pressure-induced enhancement of magnon excitations in CeCoSi, *Phys. Rev. B* **101**, 214426 (2020).
- [6] T. Hahn, ed., *International tables for crystallography*, 5th ed., Vol. A (Springer, 2005) corrected reprint of the 5th edition.